

Supporting Information for

Dynamic generation of concentration- and temporal-dependent chemical signals in an integrated microfluidic device for single-cell analysis

Alan M. González-Suárez¹, Johanna G. Peña-Del Castillo²,
Arturo Hernández-Cruz² and José L. García-Cordero^{1*§}

¹Unidad Monterrey, Centro de Investigación y de Estudios Avanzados del Instituto Politécnico Nacional, Parque PIIT, Apodaca, Nuevo León C.P. 66628, Mexico

²Departamento de Neurociencia Cognitiva y Laboratorio Nacional de Canalopatías, Instituto de Fisiología Celular, Circuito de la Investigación Científica s/n, Ciudad Universitaria, Universidad Nacional Autónoma de México, C.P. 04510 CDMX, Mexico

* Corresponding author: jlgarciac@cinvestav.mx

Contents:

Materials	S-3
Microfluidic device fabrication.....	S-3
Experimental setup.....	S-4
Table S1. Comparison between our device and previously reported devices to analyze single cells under different conditions.....	S-5
Fig. S1. Microfluidic device design.....	S-6
Fig. S2. Simulation of 2D shear-stress on cells positioned at different heights inside microwells.....	S-6
Table S2. Maximum shear stress at different inlet flow rates on cells located at different heights in the microwells	S-7
Fig. S3. Characterization of the concentration gradient generator (CGG).....	S-7
Fig. S4. Normalized concentration gradient profiles generated in each chamber at different flow rates	S-8
Fig. S5. Characterization of the time required to exchange a solution in sections of a microchamber	S-8

Fig. S6. Single-cell analysis using Matlab.	S-9
Fig. S7. Graph of the mean fluorescence intensity over time measured in each of the nine chambers for calcein-AM staining	S-10
Fig. S8. Single-cell calcein-AM response at each chamber	S-11
Table S3. Gaussian fit parameters for histograms in Fig. S7.....	S-12
Fig. S9. Single-cell responses to carbachol stimulation at 4.5 mHz	S-12
Fig. S10. Periodic stimulation of HEK-293 cells with carbachol at 20 mHz	S-13
Fig. S11. Single-cell responses to carbachol stimulation at 20 mHz	S-14
Supplementary Movies.	S-14
References	S-15

Materials

Dulbecco's modified eagle medium (DMEM)/F/12 nutrient mixture (11320033), fetal bovine serum (FBS, 16000044), penicillin-streptomycin solution (15140-122), Dulbecco's phosphate buffered saline (PBS, 21300-058), TrypLE express enzyme (1X, 12604013) were obtained from Gibco Life Technologies (USA). Dextran tetramethylrhodamine 40 kDa (dextran-rhodamine, D1842) and Calcein-AM from Molecular Probes (USA). Fluo-8-AM esters (21080) and Pluronic F-127 (20052) from ATT Bioquest. Caffeine (C-0750), carbamoylcholine chloride (carbachol, C4382), HEPES (H4034), D-glucose (G7528), fluorescein isothiocyanate isomer I (FITC, F7250), magnesium chloride (solution 1.0M, 63020), potassium hydroxide (35113), sodium hydroxide (32255, Fluka), sodium phosphate monobasic (S-5011) and sodium phosphate dibasic (S-5136) from Sigma Aldrich (USA). Calcium chloride (1313-01), potassium phosphate dibasic (3252-01), sodium bicarbonate (3506-01) and sodium chloride (3624-01) from J.T. Baker by Fisher Scientific (USA).

Materials for fabrication included negative photoresist (GM1060, Gersteltec Sàrl), positive photoresist (AZ9260 Microchem, USA) and polydimethylsiloxane (PDMS, Sylgard 184, Dow Corning, USA).

Microfluidic device fabrication.

The microfluidic device was fabricated by multi-layer soft lithography and consists of a flow and a control layer, and a third layer consisting of microwells together with the gradient generator (μ wells-CGG) layer. A separate mold was produced for each layer. Three silicon wafers (test-grade, Desert Silicon Inc., USA) were cleaned in oxygen plasma for 10 min in a plasma system (Zepto, Diener Electronic GmbH, Germany). Two of the wafers were then coated with negative photoresist (GM-1060, Gersteltec, Switzerland) to a height of 20 μ m and soft-baked on a hot plate. Next, the wafers were exposed with a micropattern generator (μ PG 101, Heidelberg Instruments, Germany) with their respective CAD design, followed by a post-bake with the exact same parameters as the soft-bake. The wafers were developed using PGMEA (484431, Sigma Aldrich, USA). Finally, the molds were baked at 135°C for 2 h.

For the flow mold, a different wafer was first spin-coated with an adhesion promoter (ADP, Gersteltec, Germany) and then spin-coated with positive photoresist (AZ 9260, Clariant, USA) at 1800 rpm for 40 s, and soft-baked at 90 °C for 1 min and 115 °C for 3 min. To reach a height of 25 μ m, a second layer of photoresist was spin-coated with the same parameters, but this time with a soft-bake step of 1 min at 90 °C and 6 min at 115 °C. The mold was exposed with the micropattern generator and developed on AZ-400K developer (AZ Electronic Materials, USA).

Finally, to reflow the photoresist the wafer was placed on an oven for 2 h at 135 °C. All molds were exposed to chlorotrimethylsilane for 30 min in a vacuum desiccator.

To make PDMS replicas of the mold, a thin layer (~50 µm height) of PDMS (20:1 ratio) was spin-coated on top of the flow layer at 1400 rpm for 40 s, while a mixture of PDMS (5:1 ratio) was poured on the control layer to reach a height of 3-4 mm. After 30 min, both molds were baked at 80°C for 25 min. Next, the control layer was peeled off, devices cut out, and holes were punched out. The control replicas were manually aligned over the flow layer mold. Then, both layers were baked together for 90 min at 80°C. The multilayer devices were peeled off from the flow mold and holes punched out. Replicas were covered with magic tape before alignment with the µwells-CGG layer.

The PDMS replica of the µwells-CGG mold was fabricated by pouring PDMS (10:1 ratio) in this mold to a height of 3-4 mm, baked for 1h at 80 °C, and peeled off from the mold. Then, the flow/control device was placed on top of a clean silicon wafer with the microchannels facing up. The µwells-CGG PDMS-replica was manually aligned on top of it under a stereomicroscope. Finally, this three-layer device was baked for 48 h at 80 °C to ensure a strong bonding between all the PDMS layers.

Experimental setup

At the beginning of each experiment, the microchannels in the control layer were filled with DI water. Pluronic F-127 0.02% w/v in PBS 1X was flowed in the flow-layer microchannels for 15 min, before being washed with PBS or Krebs HEPES solution until the experiment began.

Fluid flow was controlled through a custom-made pneumatic system that comprises 36, 3-way solenoid valves (model MH1, Festo, Germany), an Arduino Mega 2560 (Arduino, USA), flow regulators and manometers. Solenoid valves are controlled with a PC through a LabVIEW interface (National Instruments, USA). We used a using an inverted epifluorescence microscope, equipped with a dry Leica 10X/ 0.25 NA Hi PLAN objective and a set of fluorescent filter sets: L5 (ex BP 480/40 nm, dichromatic mirror 505 nm, and em BP 520/30) and N3 (ex BP 546/12 nm, 565 nm, em BP 600/40). Images were acquired using a CCD digital camera (DFC320; Leica Microsystems).

A limitation of our experimental setup is the time it takes for the motorized stage, using a 10x objective, to find a new position, take a picture, move from one microchamber to the next, and so on. Acquiring a complete set of images of the device microchambers takes ~15 s (1.6 s per

chamber). This is the peak time resolution of our system to monitor cellular responses to a complete set of agonist concentrations. This time could be further reduced by decreasing the size of the microchambers and the number of microwells in it, albeit at the cost of stimulating less cells.

Table S1. Comparison between our device and previously reported devices to analyze single cells under different conditions.

The following table contains the key features of microfluidic devices used to study single-cell dynamics. References were reduced to living cells and cell signaling studies. All devices that rely on cell adhesion for cell trapping can't be used with non-adherent cell types, and number of cells trapped is always changing and not specific. Droplet microfluidics and organoids were not considered.

Year	Ref	Cell type	Study	Trapping method	Total number cells per chip	Pulsing	Max freq. [mHz]	Shear stress [dyne/cm ²]	Parallel concentration stimulation	No of independent channels
2010	1	HEK-293	Ca ²⁺ dynamics	Hydrodynamic traps and cell adhesion	≈35	✓	≈333	NR	✗	N/A
2013	2	HEK-293	Ca ²⁺ dynamics	Hydrodynamic traps	≈100	✓	≈333	NR	✗	N/A
2014	3	Jurkat	Ca ²⁺ dynamics	Micropores and chambers	1,000	✓	250	<10	✗	N/A
2015	5	Jurkat	H ₂ O ₂ and Ca ²⁺ dynamics	Hydrodynamic traps	≈4,000 (50 cells measured)	✓	10	0.3 - 2	✓	3
2016	6	RAW 264.7	Cytokine secretion	Hydrodynamic traps	40	✓	100	NR	✓	40
2017	7	Jurkat	H ₂ O ₂ and Ca ²⁺ dynamics	Hydrodynamic traps	1,000 (≈600 analyzed)	✓	16.7	<10	✗	N/A
2017	8	3T3	NF-κB activity	Cell adhesion	Not mentioned (50 analyzed)	✓	100	Low (NR)	✗	N/A
2017	9	RAW 264.7	NF-κB activity and cytokine secretion	Hydrodynamic traps	From 16 to ≈600	✓	100	NR	✓	16
2017	10	3T3	Ca ²⁺ dynamics	Cell adhesion	Not mentioned	✓	50	NR	✗	N/A
2018	11	HMVEC-d, HeLa, U-251	Ca ²⁺ dynamics	Cell adhesion	>200 (50 analyzed)	✓	500	NR	✗	N/A
This work		HEK-293	Ca²⁺ dynamics	Microwells	4,428	✓	33.3	0.551	✓	9

NR = Not reported, N/A not available

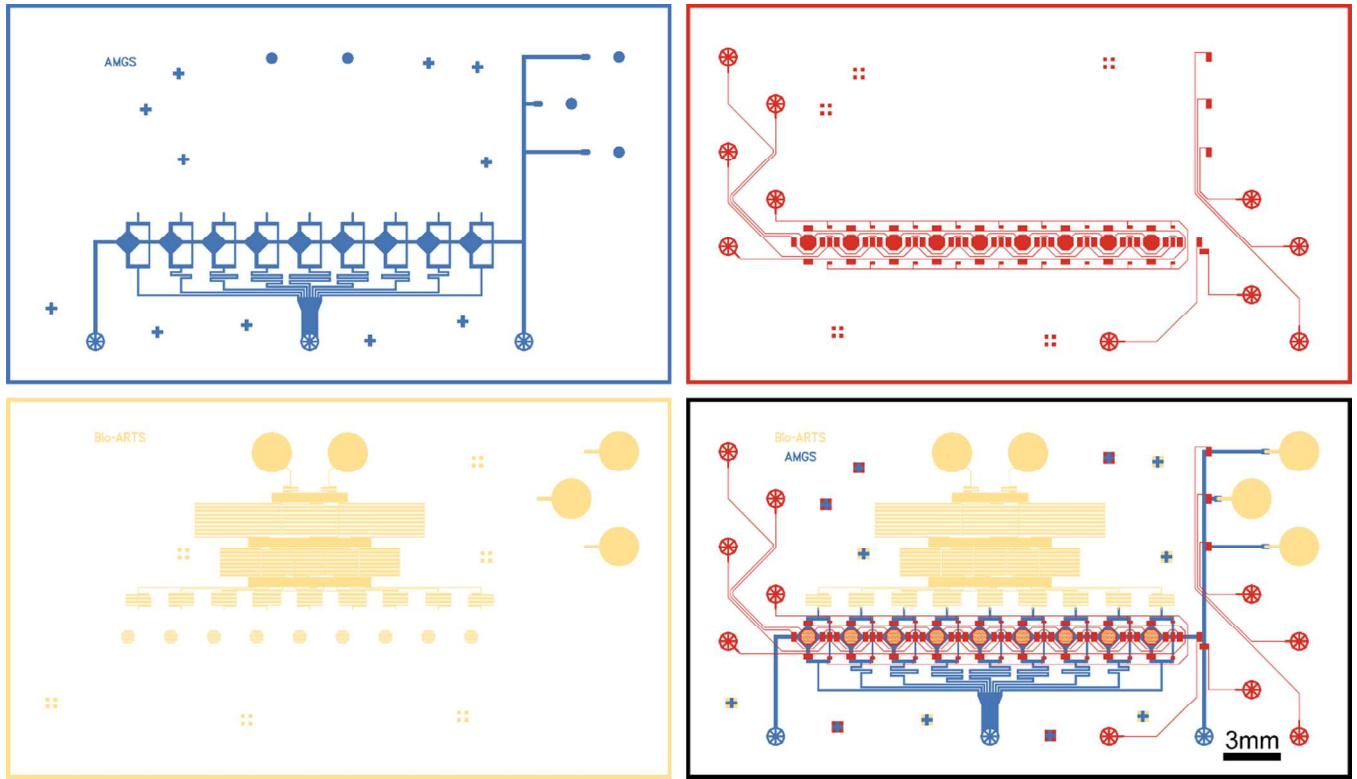


Figure S1. Microfluidic device design. Each color represents a different layer: blue and yellow color represent the flow layers; the gradient generator is embedded in the yellow layer. The red color denotes the control layer. The integrated layers are shown in the bottom right figure.

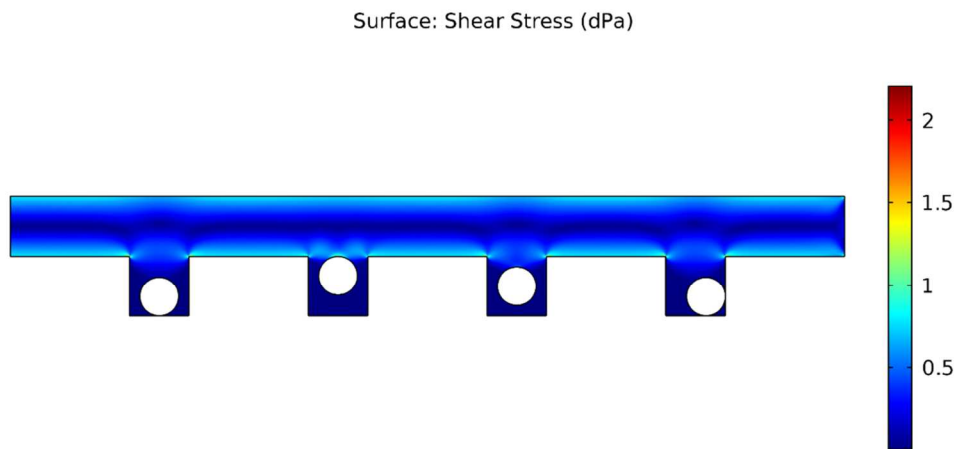


Figure S2. Simulation of 2D shear-stress on cells positioned at different heights inside microwells. Cells are represented by white circles. A flow rate of $0.222 \mu\text{L}/\text{min}$ was used. Color bar indicates the shear stress value. $1 \text{ dPa} = 1 \text{ dyne}/\text{cm}^2$.

Table S2. Maximum shear stress at different inlet flow rates on cells located at different heights in the microwells. Microchannel volumetric flow = 1/9 of the main inlet volumetric flow.

Inlets volumetric flow [$\mu\text{L}/\text{min}$]	Chamber volumetric flow [$\mu\text{L}/\text{min}$]	Shear stress [dyne/cm^2]			
		Bottom	Top	Middle	Corner
1.0	0.111	0.064	0.583	0.276	0.051
2.0	0.222	0.128	1.164	0.551	0.102
3.0	0.333	0.192	1.748	0.826	0.153
4.0	0.444	0.256	2.330	1.102	0.204
5.0	0.556	0.321	2.916	1.377	0.255
6.0	0.667	0.385	3.467	1.655	0.307

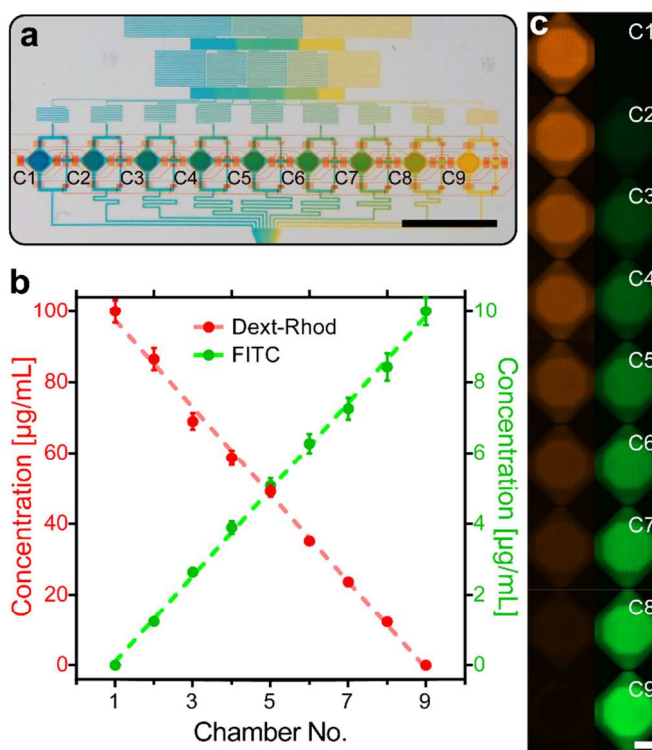


Figure S3. Characterization of the concentration gradient generator (CGG). (a) Photograph of a section of the CGG with solutions flowing into the 9 chambers (scale bar = 4 mm). (b) Graph showing the linear profile created using Dextran-Rhodamine (red) and FITC (green); $r^2 > 0.99$ in both cases. Error bars: 1 standard deviation; $n=3$. (c) Fluorescence micrographs of the 9 chambers filled with DR (left) and FITC (right) after the gradient has been formed (scale bar = 200 μm).

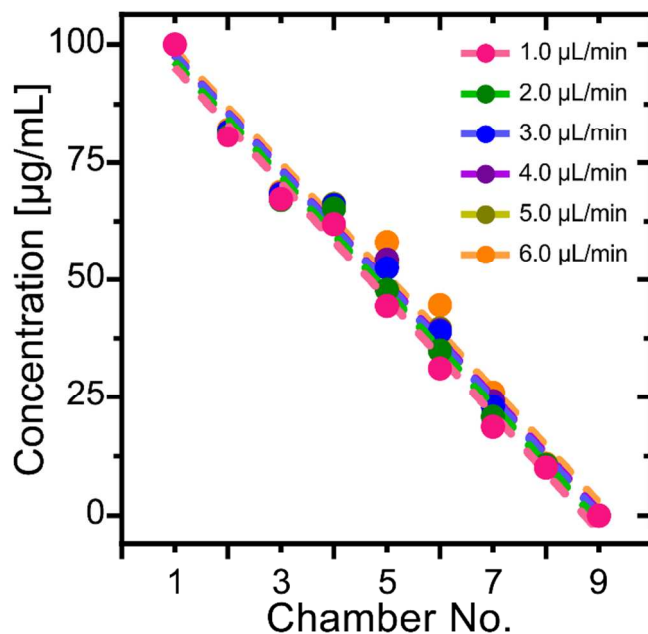


Figure S4. Normalized concentration gradient profiles generated in each chamber at different flow rates. The leftmost chamber (No.1) receives the highest concentration of Dextran Rhodamine (μM) while buffer is delivered to the rightmost chamber (No. 9). Flow rates range from 1.0 to 6.0 $\mu\text{L}/\text{min}$. R^2 is 0.99 for all the flow rates.

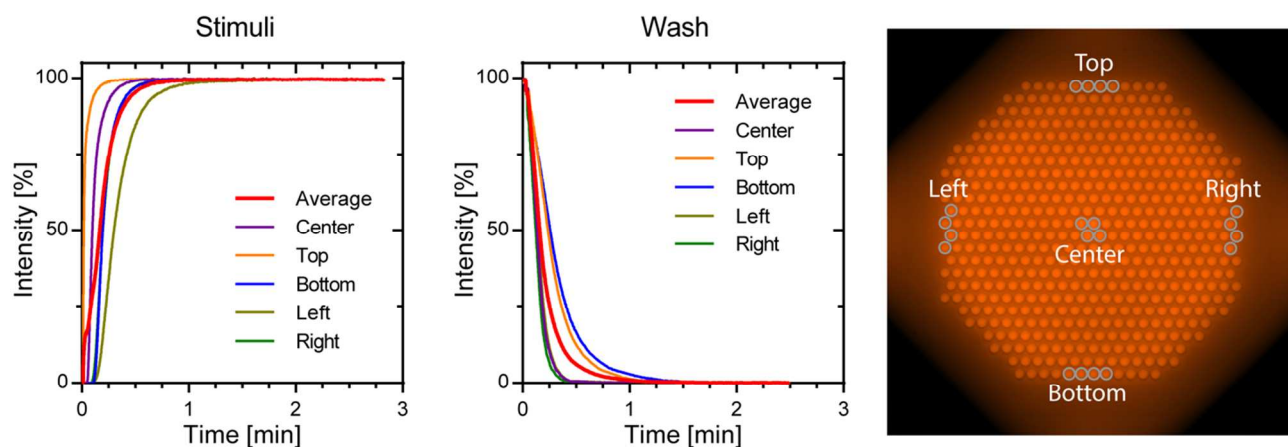


Figure S5. Characterization of the time required to exchange a solution in sections of a microchamber. We characterized time for the stimuli step (top to bottom flow in a chamber) and the washing step (left to right flow in a chamber). Right, image of a microchamber. The gray dots symbolize the locations where fluorescent measurements were acquired. Characterization was performed using a solution of Dextran-Rhodamine. Solutions were flown at 2 $\mu\text{L}\cdot\text{min}^{-1}$.

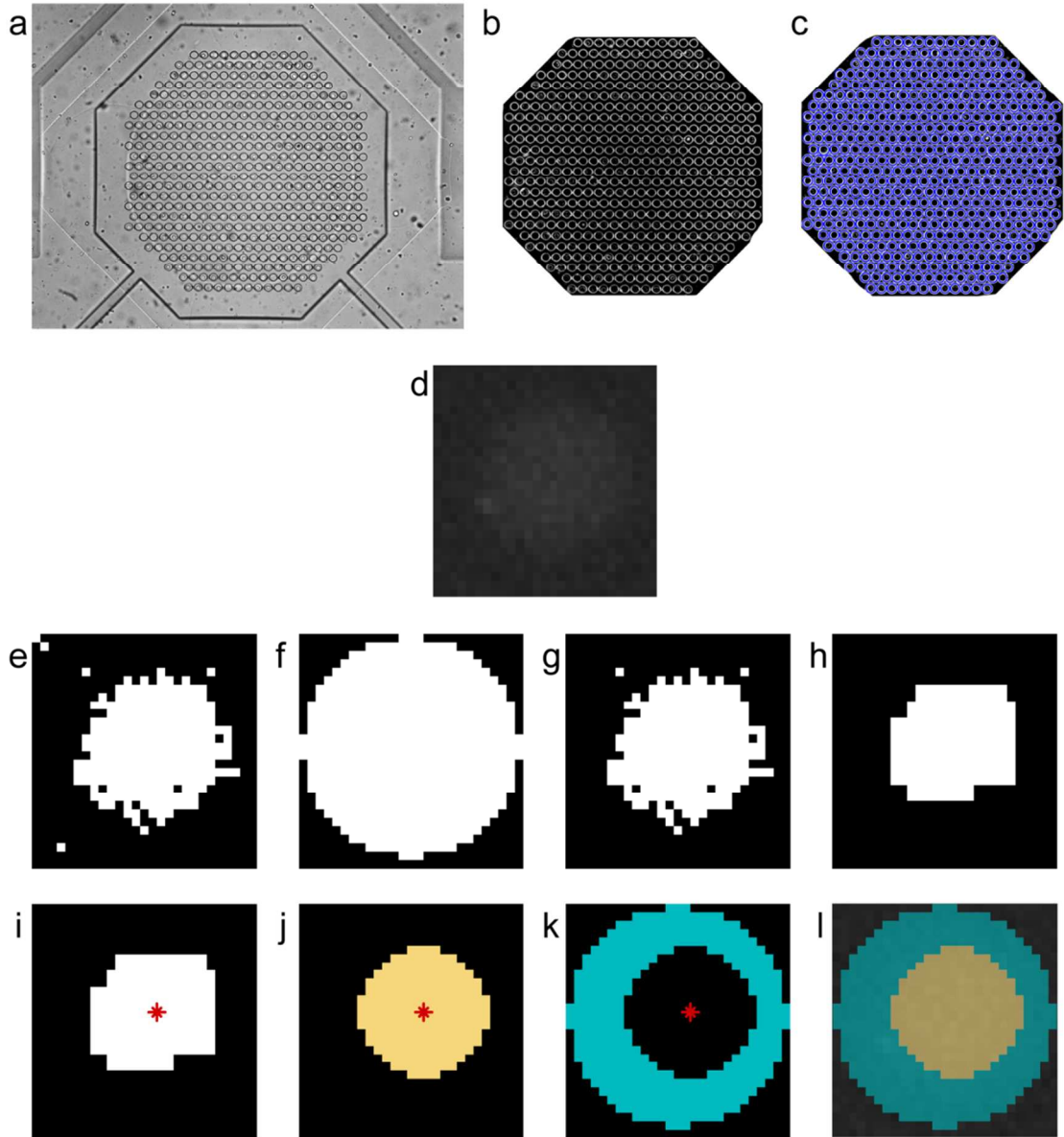


Figure S6. Single-cell analysis using Matlab. (a) A brightfield (BF) image from each chamber is taken at the beginning of each experiment. Microwell are detected on this image. (b) The BF image is manually cropped and enhanced to avoid artifacts in microwells detection using Photoshop. (c) Each cropped-BF image is opened in Matlab and microwells are automatically detected, saving the location and radius of each microwell. (d) In the first fluorescence image of the sequence, all microwells are cropped and binarized (e) to locate the cells. (f) A mask is created to remove bright pixels outside the microwell (g). (h) Erode and dilate functions are applied to remove lonely bright pixels and black areas in the object. (i) Center of mass is found, and the image is separated in two areas: a cell area corresponding to a 8 pixel radius circle (j), and the bottom of the microwell (k). (l) In the original cropped image, the average intensity of the pixels from the bottom of the microwell is subtracted from the average intensity of the cell area, and the value is saved as the fluorescence intensity of that cell in that point in time. The same process is repeated for all images of the same chamber and all of the chambers of the device. As a final

step, k-means clustering is applied to organize data and create heatmaps. Data is automatically exported to an Excel file.

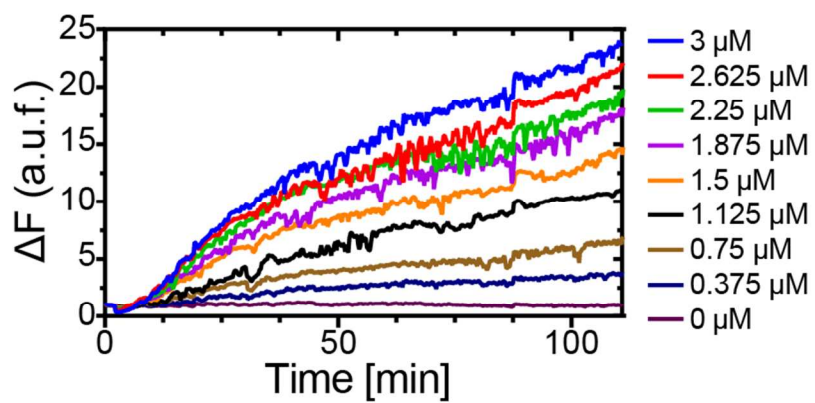


Figure S7. Graph of the mean fluorescence intensity over time measured in each of the nine chambers for calcein-AM staining.

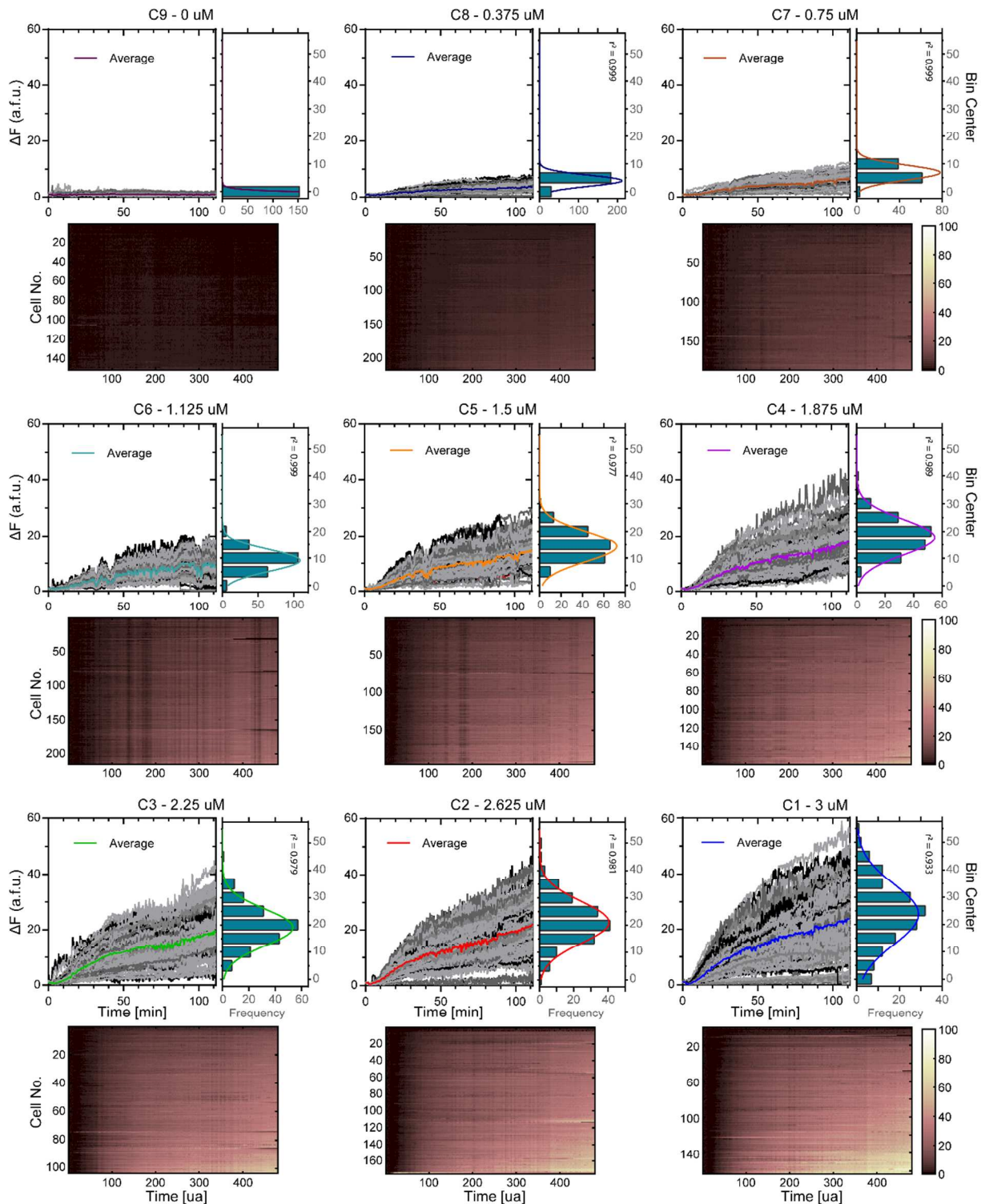


Figure S8. Single-cell calcein-AM response at each chamber. Panel shows graph curves for individual (grey lines) and average response (color lines) at each concentration. Histograms depict cell frequency of end point fluorescence intensity, and its gaussian fit. Pseudo-color maps show fluorescence intensity of each cell during the whole experiment. Gaussian fit parameters for each curve can be found in Table S2.

Table S2. Gaussian fit parameters for histograms in Fig. S7.

	C1	C2	C3	C4	C5	C6	C7	C8	C9
Amplitude	28.9	40.54	53.4	54.7	72.05	108.5	77.97	211.5	---
Mean	23.75	21.07	19.05	17.75	14.33	9.177	6.864	3.93	---
SD	11.04	7.633	6.728	6.479	5.548	3.979	2.662	1.988	---

Equation $y = Amplitude \cdot e^{-0.5\left(\frac{x-Mean}{SD}\right)^2}$

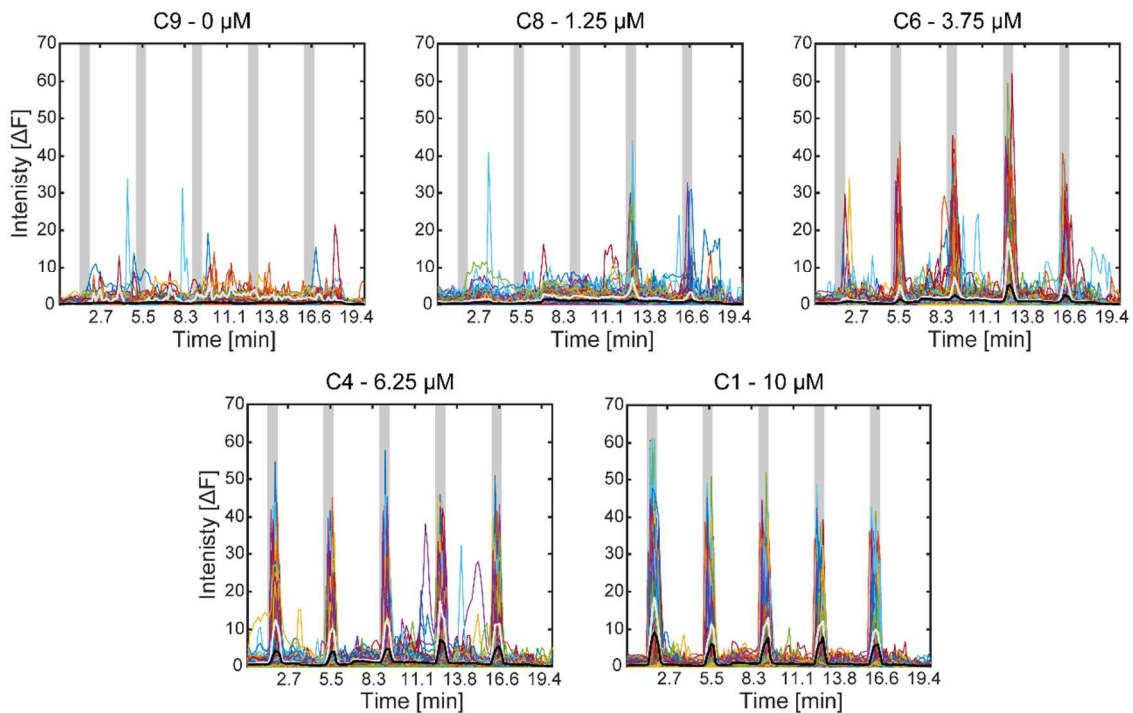


Figure S9. Single-cell responses to carbachol stimulation at 4.5 mHz. Color lines represent individual cells, black lines the average response of all cells, and white lines average of only responsive cells. Pseudo-color maps are presented in main text (Figure 4).

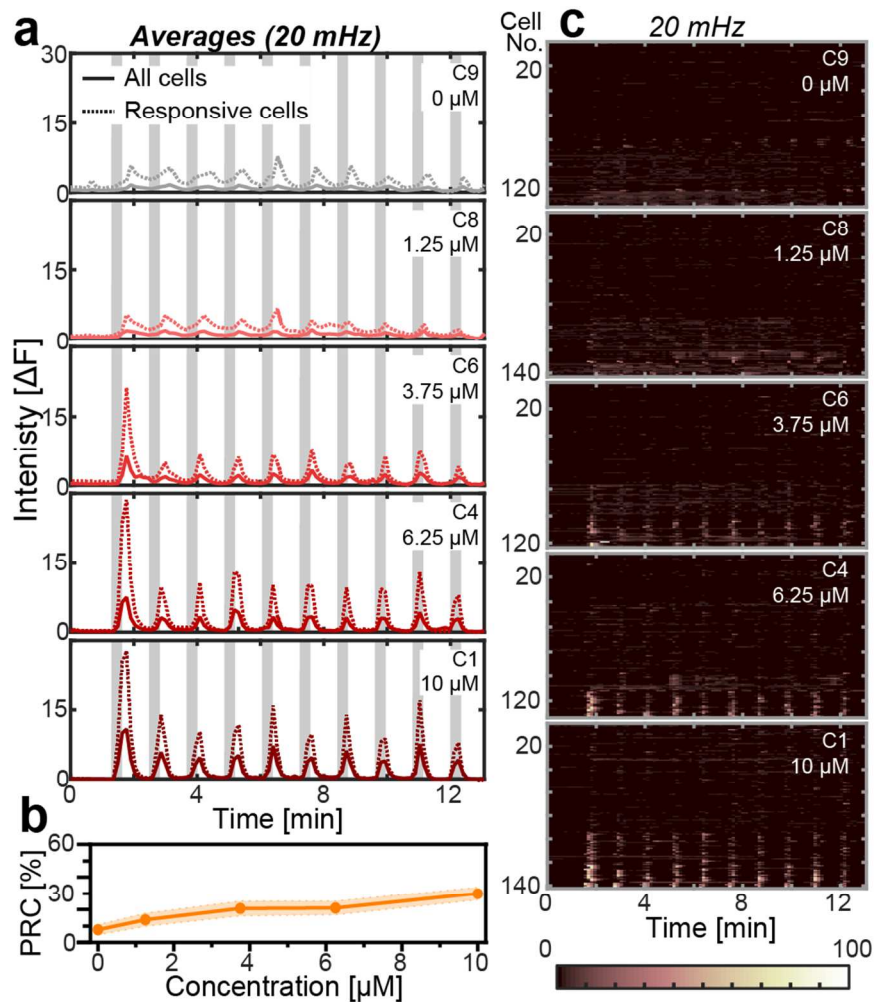


Figure S10. Periodic stimulation of HEK-293 cells with carbachol at 20 mHz. **(a)** The graph shows average responses for a group of cells stimulated at a frequency of 20 mHz. Solid lines show average response of all cells; dashed lines show average response of only responsive cells. Carbachol exposure is represented by vertical gray bars. **(b)** Graphs showing the percentage of responsive cells (PRC) for data shown in (a) at each concentration. The dimmed area around the average line shows the standard deviation. **(c)** Heat maps corresponding to single-cell analysis of data in (a) after k-means clustering, where the response of each individual cell is represented in each row for the duration of the experiment. Colormap is normalized to the data of highest concentration for each frequency.

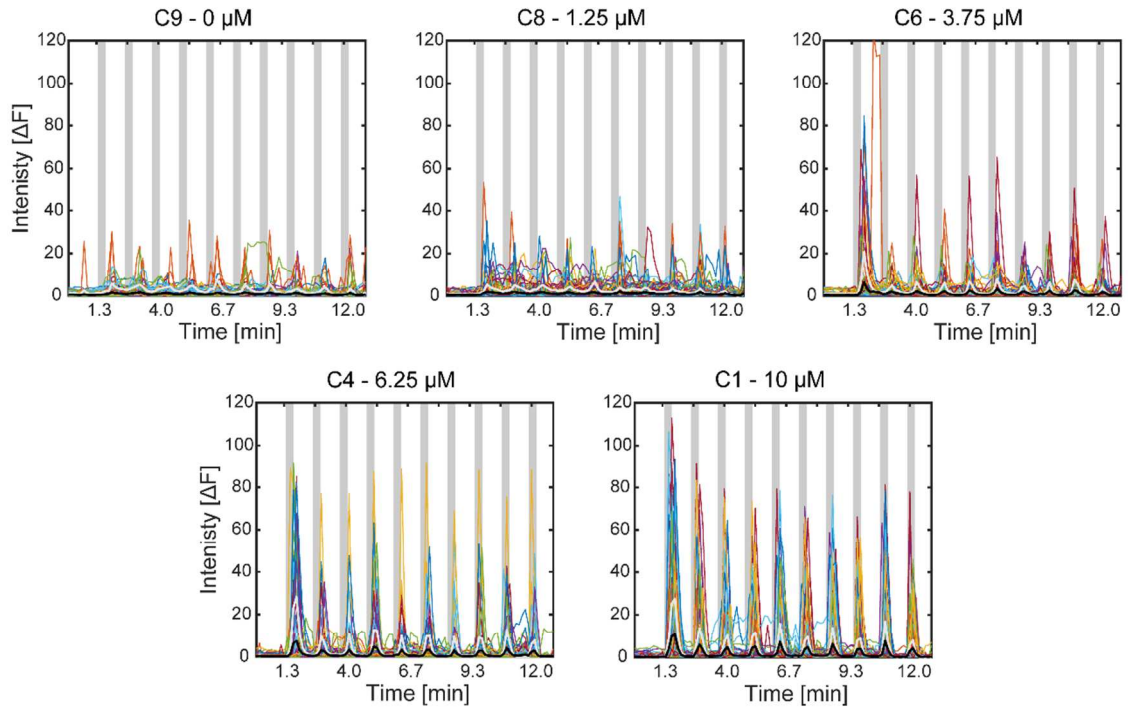


Figure S11. Single-cell responses to carbachol stimulation at 20 mHz. Color lines represent individual cells, black lines the average response of all cells, and white lines average of only responsive cells. Pseudo-color maps are presented in Figure S9.

Supplementary movies (available online)

Movie M1. Representative video of a segment where solution is exchanged in a microchamber using Dextran-Rhodamine, representing a stimulus, and PBS as washing solution.

Movie M2. Time lapse of HEK-293 cells trapped inside microwells and stimulated with carbachol 10 μ M for 10 s, followed by a washing step. Cells were previously loaded with Fluo-8 AM.

References

- 1 A. Jovic, B. Howell, M. Cote, S. M. Wade, K. Mehta, A. Miyawaki, R. R. Neubig, J. J. Linderman and S. Takayama, *PLoS Comput. Biol.*, 2010, **6**, e1001040.
- 2 A. Jovic, S. M. Wade, R. R. Neubig, J. J. Linderman and S. Takayama, *Integr. Biol.*, 2013, **5**, 932.
- 3 L. Chingozha, M. Zhan, C. Zhu and H. Lu, *Anal. Chem.*, 2014, **86**, 10138–10147.
- 4 R. A. Kellogg and S. Tay, *Cell*, 2015, **160**, 381–392.
- 5 L. He, A. Kniss, A. San-Miguel, T. Rouse, M. L. Kemp and H. Lu, *Lab Chip*, 2015, **15**, 1497–1507.
- 6 M. Junkin, A. J. Kaestli, Z. Cheng, C. Jordi, C. Albayrak, A. Hoffmann and S. Tay, *Cell Rep.*, 2016, 1–12.
- 7 A. S. Kniss-James, C. A. Rivet, L. Chingozha, H. Lu and M. L. Kemp, *Integr. Biol.*, 2017, **9**, 238–247.
- 8 A. Piehler, N. Ghorashian, C. Zhang and S. Tay, *Lab Chip*, 2017, **17**, 2218–2224.
- 9 A. J. Kaestli, M. Junkin and S. Tay, *Lab Chip*, 2017, **17**, 4124–4133.
- 10 P. Chen, Y. Guo, X. Feng, S. Yan, J. Wang, Y. Li, W. Du and B. F. Liu, *Anal. Chem.*, 2017, **89**, 9209–9217.
- 11 P.-H. Huang, C. Y. Chan, P. Li, Y. Wang, N. Nama, H. Bachman and T. J. Huang, *Lab Chip*, 2018, 531–540.